Progress in Flight Physics **7** (2015) 509-524
DOI: 10.1051/eucass/201507509

ON THE RELATIVE "RECEPTIVITY" OF TWO- AND THREE-DIMENSIONAL SUPERSONIC BOUNDARY LAYERS TO STATIONARY DISTURBANCES AT MACH 2

A. D. Kosinov, A. V. Panina, N. V. Semionov, and Yu. G. Yermolaev

Khristianovich Institute of Theoretical and Applied Mechanics
Siberian Branch of the Russian Academy of Sciences
4/1 Institutskaya Str., Novosibirsk 630000, Russia

Experiments on the influence of flat isolated square and diamond shaped roughness elements on the mean and pulsation characteristics of the boundary layer on a flat plate and a swept wing of comparable size are conducted. The shape of stickers has almost no effect on the mass flow pulsation amplitude in the trace of roughness. The relative "receptivity" of the three-dimensional (3D) boundary layer to stationary perturbations is approximately 1.5 times greater than the "receptivity" of the two-dimensional (2D) boundary layer. The presence of roughness on the disturbance source line changes the pulsation spectra in 2D/3D boundary layer compared to the spectra in boundary layer on smooth surface.

1 INTRODUCTION

The problem of the turbulence origin in the supersonic boundary layer on a swept wing has been in focus for researchers for more than 50 years [1–6]. Recently, the problem of boundary layer transition has received increasing attention. For high supersonic speeds, the important issue is the thermal protection of vehicle designed for entry into the atmosphere. It is well known that heat transfer in the laminar boundary layer is much smaller than in turbulent boundary layer. Thus, the relevance of predicting the transition position and flow laminarization in the boundary layer is only growing. However, both of these problems are far from being solved. Existing methods of the laminar flow control in the boundary layers are not simple to use.

Development of the transition control methods in supersonic boundary layers is technically difficult and expensive task, even for scientific research. Now, the method of the flow laminarization with the help of microroughness on the swept wing is applied, but historically, the development of this control method began at the ITAM SB RAS. In 1985, the phenomenon of the unstable wave autodestruction in the boundary layer at subsonic flow was discovered [7]. This phenomenon radically altered the existing ideas about the role of surface roughness in the laminar–turbulent transition. It has been shown that at certain geometry, microroughness can delay the transition compared to a smooth surface. Recently, this idea has been applied to the transition control of the supersonic boundary layers on the swept wing and it has been associated with the passive method of the laminar flow control in 3D boundary layer with the help of a distributed microroughness on the surface of the swept wing near the leading edge [8].

To solve the problem of the laminar flow control, it is necessary to find out the mechanisms of boundary layer transition in detail. If the issues of stability of the laminar boundary layer at subsonic speeds were studied thoroughly in both experimental and theoretical papers [5, 9], for supersonic speeds these problems are less investigated [1–6, 10]. It should be noted that in the last years, the study of the stability of compressible boundary layers has been successful concerning the nonlinear wave interaction [11–15]. It is possible to indicate the results of numerical simulation in applying 2D roughness element for transition control in boundary layer at high supersonic speed [16]. Recent advances of numerical simulation for roughness-induced transition in high supersonic boundary layer are reviewed in [17].

As a rule, the phenomenon of the turbulence origin in the boundary layers is studied in ideal conditions, such as on smooth surfaces. However, the surfaces of the real aircraft are not perfectly smooth. The roughness height on the wing of the aircraft is up to 100 μm [8]. For application of the active or passive methods for control of transition or friction on the surface, it is necessary to consider that actuators can be installed in nonideal conditions, and their effectiveness may be different, including the changing of the characteristics of the flight. Therefore, the study of features of disturbance generation by controlled actuators to create a technology control of the transition or the surface friction of the aircraft is relevant.

It should be emphasized that without the knowledge of the transition mechanisms, it is not possible to create effective flow control methods for transition. In this case, the results of the stability theory, which use the wave approach in the description of turbulence origin, are particularly important, as in the experiments where the method of the controlled perturbations is applied. However, up to now, the investigation of the supersonic boundary layer stability is focused on the study of the development of controlled pulsations, excluding the effect of possible flow nonuniformities.

Recently extensive theoretical and experimental studies of flow control methods in boundary layers with roughness were conducted [8, 18–25]. In theory, the optimal disturbance approach is used for the analysis of the disturbed flow behind roughness on the surface [19–21]. In some works, the calculations are performed by direct numerical simulation [24]. The effectiveness of the periodic roughness to control the laminar–turbulent transition and friction characteristics of turbulent boundary layers were verified in experimental studies [14, 15, 21–23, 25, 26].

Initially, the influence of surface roughness on the stability of compressible boundary layers has been studied in models of swept wing, as these studies are of considerable practical character. In [8,23], it is shown that the periodic roughness located near the leading edge of the swept wing can stabilize boundary layer, as well as it can accelerate the laminar–turbulent transition. The flow stabilization was caused by the impact of the distributed roughness to the stationary crossflow instability. In [27], the latest results of experimental studies of laminar–turbulent transition of a supersonic boundary layer on a flat plate, the swept cylinder, and the transition flow control in the boundary layer of the swept wing with distributed microroughness made in the ITAM SB RAS are presented.

The principal limitation of flow laminarization by the surface roughness is the instability of Tollmien–Schlichting waves. Obviously, the detection of the stabilizing effect from the roughness for this mode can increase the transition Reynolds number when using the transition flow control. Let note that in experiments described in [28], which were carried out using controlled perturbations, it was shown that the packet of Tollmien–Schlichting waves can be stabilized by the periodic mean flow modulation induced by the roughness height of 60 μm. It has been also shown that the location of labels relative to the disturbance source aperture has different influence to the mean flow characteristics and to the initial controlled disturbance amplitude. An additional mean flow distortion was found [29], if the aperture was in the sticker wake. This effect certainly requires further investigation, as it may limit the development of future transition flow control technologies at supersonic speeds.

In the first experiments [15], the development and interaction of unstable waves in a modulated supersonic boundary layer on a flat plate by rectangular/square stickers were studied. To transfer this method to the swept wing boundary layer, the square stickers were placed parallel to the leading edge; so, their shape became diamond-like with respect to the external flow. Since the sticker shape has influence on the mean flow distortion, the comparison of the flow characteristics behind the same roughness in 2D and 3D boundary layers, is relevant.

The goal of this paper was to experimentally study the influence of flat microroughness with square and diamond shape on the average and pulsation characteristics of natural disturbances in the 2D and 3D supersonic boundary layers and to compare the generated flow nonuniformities in these flows, taking into account the influence of the disturbance source aperture.

2 EXPERIMENTAL SETUP

The experiments were performed in a low-noise supersonic wind tunnel T-325 of ITAM SB RAS at Mach 2 and unit Reynolds number $\mathrm{Re}_1 = 5 \cdot 10^6$ m^{-1}. A model of flat steel plate with a sharp leading edge and an aluminum model of a swept wing with a sweep angle $\chi = 45°$ were used in the experiments. After polishing, the flat plate had a near perfect flat surface and an aperture diameter of 0.5 mm for the disturbance source [11]. The aperture coordinates on the plate are $x = 37 \pm 0.25$ mm and $z = 0$ (here, x is the distance from the leading edge and $z = 0$ corresponds to the centerline of the model symmetry). Swept wing model was plane-convex profile and contained a disturbance source aperture of 0.41 mm in diameter [29]. The aperture coordinates on the working surface of the swept wing are $x = 57.7 \pm 0.25$ mm and $z = 0$.

For the generation of controlled stationary disturbances in the boundary layer a single flat surface roughness is used. They are referred to [24] "symmetrical square roughness." Thickness roughness was 60 μm. Experimental setup is shown with four variations in Fig. 1. For cases I and II, the roughness covered the aperture and was placed at $x = 37$ mm. The boundary layer thickness at the roughness installation was $\delta_{U_{0.995}} \approx 0.6$ mm. For cases III and IV, the roughness element did not cover the aperture, and there was a combined effect

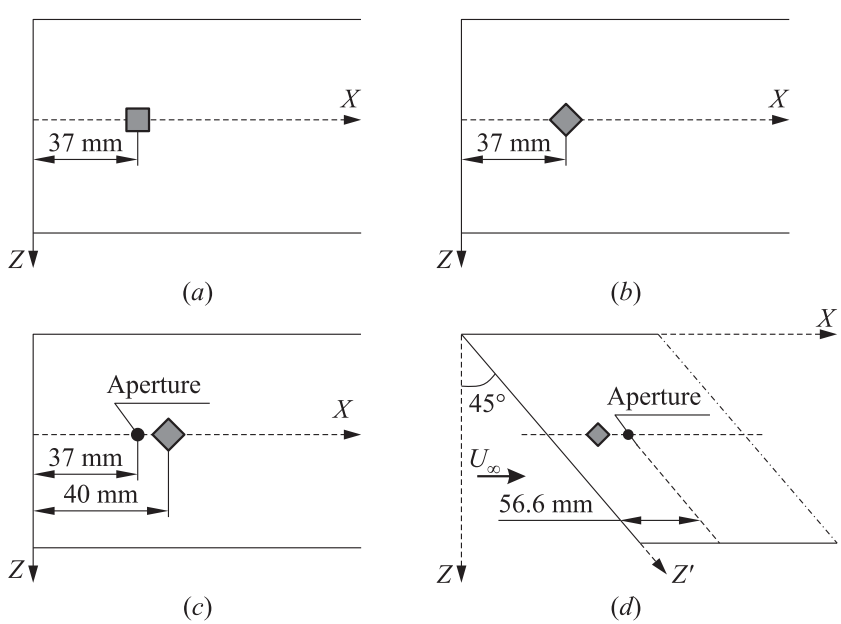

Figure 1 The experimental setup: (*a*) case I; (*b*) II; (*c*) III; and (*d*) case IV

of roughness and aperture to the mean flow structure downstream. The distance from the leading edge to the surface roughness was chosen so that the boundary layer thickness at the roughness location on the flat plate and swept wing had the same boundary layer thickness (i. e., $\delta_{U_{0.995}} \approx 0.7$ mm). Natural disturbance measurements were in the section where the local thickness of the boundary layer was $\delta_{U_{0.995}} \approx 1$ mm in all cases of the stickers location (at a distance $x = 96.5$ mm from the leading edge of the line discharge on the wing and at the distance $x = 76.5$ mm from the leading edge — the plate).

The disturbances in the flow were measured by constant temperature hot-wire anemometer (HWA). Hot-wire probe was made from a tungsten wire of 10 μm in diameter and of 1.5 mm in length. With the help of the traversing gear, the probe was moved in x, y, z directions. Accuracy of sensor locating in x, z directions was 0.1 mm, and it was 0.01 mm for y. At the probe movement along the transverse coordinate, the flow pulsation measurements were carried out at $x = const$ and $y = const$. The wire overheat ratio was installed about 0.8; so, the measured disturbances consisted from mass flow pulsations on 95% [30].

The mean voltage E of output signal from the HWA was measured with a digital voltmeter Agilent 34401A. Pulsations of output signal from the HWA were digitalized by 12-bit analog-to-digital converter (ADC) with sampling frequency of 750 kHz and then recorded to the computer memory.

To determine the character of natural disturbance evolution in the boundary layer, a statistical approach was used which allowed one to define the linear and nonlinear pulsation development [31].

To determine the mean flow distortion, the relative change of the average mass flow in the spanwise direction was used. The procedure can be obtained by using the relation between the mean voltage output from the anemometer and the mean mass flow [30, 32]:

$$E^2 = L + M(\rho U)^n \,. \tag{1}$$

Let take the differential from Eq. (1):

$$d\left(E^2\right) = d\left(L + M(\rho U)^n\right) \,.$$

The following is obtained:

$$2E\,dE = Mn(\rho U)^{n-1}\,d(\rho U)\,.$$

Dividing the left side by E^2 and the right by $L + M(\rho U)^n$ and neglecting of L due to the procedure described in [30], one obtains:

$$2\,\frac{\Delta E}{E} \approx n\,\frac{\Delta(\rho U)}{\rho U}\,. \tag{2}$$

According to the results of sensor calibration, n is about 0.5; so, expression (2) can be rewritten as

$$\frac{\Delta(\rho U)}{\rho U} \approx 4\,\frac{\Delta E}{E}\,. \tag{3}$$

The mass flow pulsation oscillograms m' measured by hot-wire was normalized on the local value of the mean mass flow similar to Eq. (3) [30].

3 RESULTS

The results of the distribution measurements mean and fluctuating mass flow characteristics behind the roughness in z direction at different y are shown in Figs. 2–5. Figures 2a–5a show the defect of the relative amplitude values of the

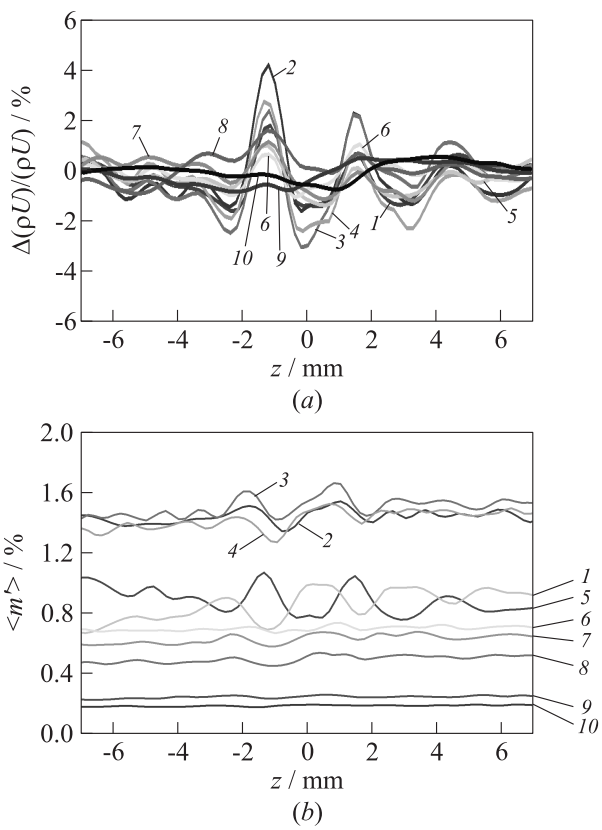

Figure 2 Case *I*: normalized distributions of mean flow distortions (a) and distributions of total mass flow pulsations (b) in the wake of a single roughness over z at different y: *1* — 0.51 mm; *2* — 0.56; *3* — 0.61; *4* — 0.66; *5* — 0.71; *6* — 0.76; *7* — 0.81; *8* — 086; *9* — 0.91; and *10* — 0.96 mm

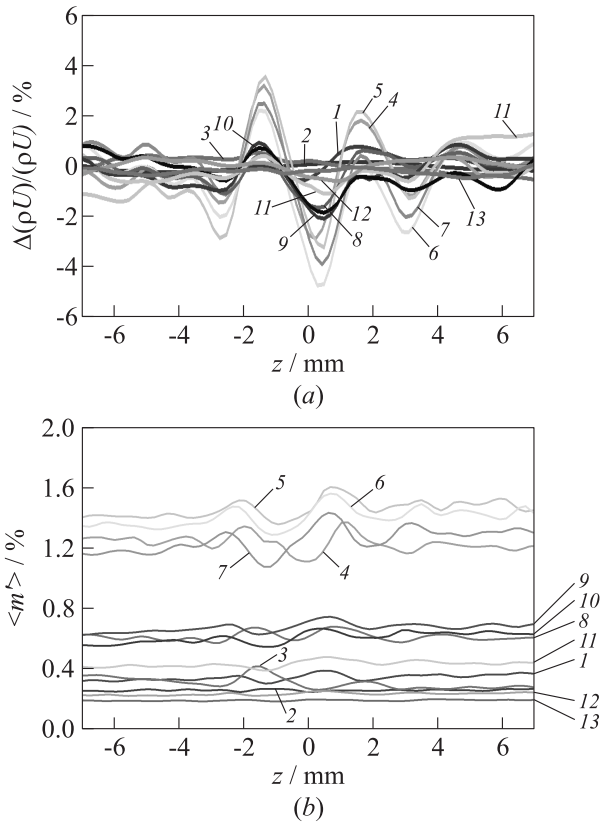

Figure 3 Case *II*: normalized distributions of mean flow distortions (*a*) and distributions of total mass flow pulsations (*b*) in the wake of a single roughness over z at different y: *1* — 0.39 mm; *2* — 0.44; *3* — 0.50; *4* — 0.54; *5* — 0.60; *6* — 0.66; *7* — 0.71; *8* — 0.76; *9* — 0.81; *10* — 0.86; *11* — 0.91; *12* — 0.96; and *13* — 1.03 mm

mean mass flow obtained according to the relation (3). The data for cases *I* (see Fig. 2*a*) and *II* (see Fig. 3*a*) allow to suggest that the diamond-shaped sticker creates a large defect in the normal direction to the surface compared with a flat square roughness. However, the maximum distortion in both cases is approximately the same and equals about ±4%. Maximum defect for the normal direction is associated with median area of the roughness. The results for cases *III* (see Fig. 4*a*) and *IV* (see Fig. 5*a*) confirm the last conclusion as 2D and 3D boundary layers. The maximum mean flow distortion is increased behind apertures in the model surface in the case *III* from +5% to −13% (see Fig. 4*a*) and in the case *IV* from +11% to −14% (see Fig. 5*a*). The mean flow distortion for smooth models was approximately ±1.5% and associated with

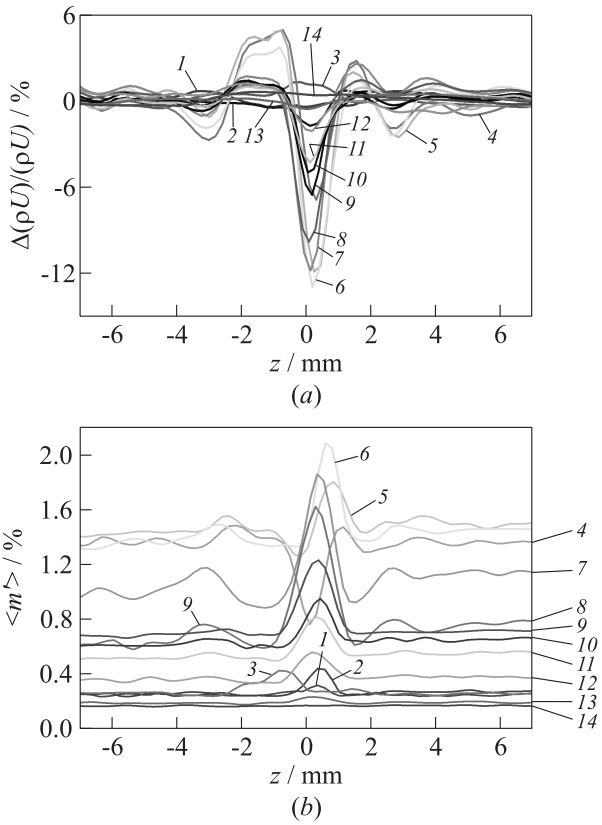

Figure 4 Case *III*: normalized distributions of mean flow distortions (*a*) and distributions of total mass flow pulsations (*b*) in the wake of a single roughness over z at different y: *1* — 0.20 mm; *2* — 0.26; *3* — 0.31; *4* — 0.37; *5* — 0.42; *6* — 0.47; *7* — 0.51; *8* — 0.55; *9* — 0.59; *10* — 0.62; *11* — 0.77; *12* — 0.73; *13* — 0.84; and *14* — 0.91 mm

accuracy maintaining the flow regime of T-325. Note that the minimum average error in determining the mass flow from hot-wire data in the boundary layer cannot be better than 1%. It can be argued that the presence of apertures in the smooth models did not introduce significant additional mean flow distortions in the transverse direction.

Figures 2*b*–5*b* show the distribution of total mass flow pulsations across the boundary layer at different distances from the model surface. Spanwise mean flow nonuniformity changes background natural disturbances in the wake of stickers. It remains uniform in average for smooth models in spanwise direction. For cases *I* (see Fig. 2*b*) and *II* (see Fig. 3*b*) in the wake of the roughness, background becomes nonuniform in vicinity of ±10% from average value

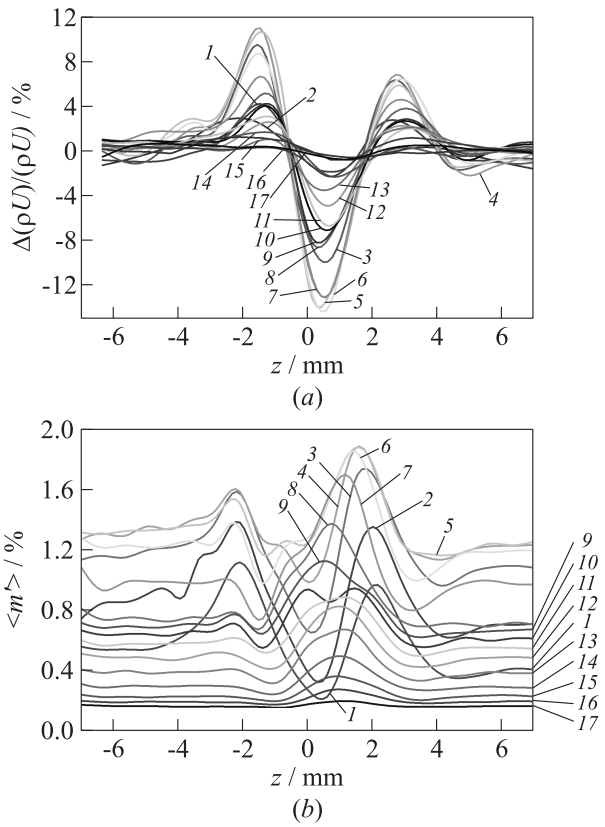

Figure 5 Case *IV*: normalized distributions of mean flow distortions (*a*) and distributions of total mass flow pulsations (*b*) in the wake of a single roughness over z at different y: *1* — 0.45 mm; *2* — 0.48; *3* — 0.51; *4* — 0.54; *5* — 0.57; *6* — 0.61; *7* — 0.64; *8* — 0.67; *9* — 0.70; *10* — 0.74; *11* — 0.77; *12* — 0.81; *13* — 0.85; *14* — 0.89; *15* — 0.93; *16* — 0.97; and *17* — 1.02 mm

of mass flux in spanwise direction for each fixed y position. Background total mass flow pulsation nonuniformity increases in several times for cases *III* (see Fig. 4*b*) and *IV* (see Fig. 5*b*). The presence of apertures in the model surface leads to a strong increase in the root mean square (RMS) pulsation amplitude above the natural maxima across the boundary layer that is formed by the instability of uniform flow for the case *III* (see Fig. 4*b*). However, in 3D boundary layer (case *IV*), the nonuniformity of natural pulsation distribution presents both above and below the natural maxima across the boundary layer (see Fig. 5*b*). Perhaps, there is the influence of the aperture location relative of stickers.

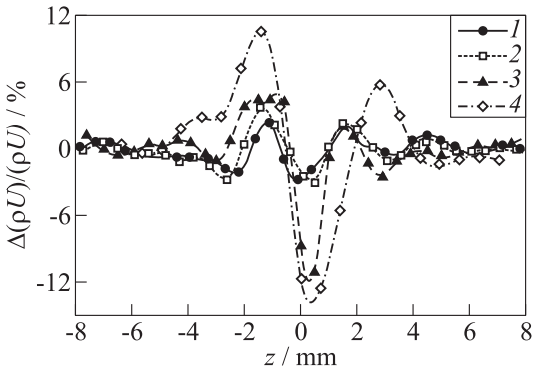

Figure 6 Comparison of the average flow distortion in the spanwise direction in the vicinity of the fluctuation maximum in the boundary layer: *1* — case *I*; *2* — *II*; *3* — *III*; and *4* — case *IV*

Comparison of the spanwise distribution of mean flow distortion in the wake of the roughness is presented in Fig. 6. The comparison is performed in the layer of maximum mass flow pulsations in the undisturbed flow. Minimum in these distributions corresponds to the sticker center, and the maxima of the mean flow distortion correspond to approximately the sticker edges. The results confirm the conclusion that the aperture has a strong influence on the mean flow defect in the wake of the roughness. In the case of "sticker plus aperture" on the flat plate (case *III*), the maximum distortion of the mean flow (peak-to-peak) is two times greater than that for the "no aperture" case on the flat plate (case *II*). Furthermore, it can be concluded that the relative "receptivity" of the 3D boundary layer to the stationary perturbations (case *IV*) is about 1.5 times higher than the "receptivity" one of 2D boundary layer (case *III*). Coordinates z (or z' for the case *IV*), corresponding to the maxima and minima of the distributions, are shown in Table 1.

The spanwise distributions of the total RMS values of mass flow fluctuations corresponding to its maxima across the boundary layer on the flat plate and on the swept wing with the stickers are shown in Fig. 7. It was found that the mass

Table 1 Z-coordinates of the maxima and minima of the mean flow distortion

Case	1st maximum, mm	2nd maximum, mm	Minimum, mm
I	−1.3	1.7	0.0
II	−1.5	1.5	0.5
III	−1.5	1.5	0.3
IV	−1.4	2.8	0.5

flow pulsations in the undisturbed flow over the flat plate was approximately 15%–20% greater than that in the case of the swept wing. It can be concluded that the label shape does not effect absolute changing of mass flow pulsations in the wake of a sticker (cases I and II). It was found that the relative variation of mass flow pulsations on the swept wing is 1.5 times higher than that on the flat plate.

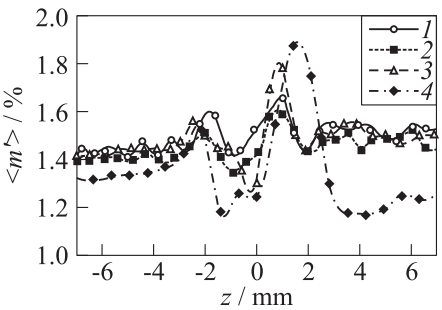

Figure 7 Comparison of the total value of mass flux amplitude in the spanwise direction: *1* — case I; *2* — II; *3* — III; and *4* — case IV

Quantitative results from the distortion of the mean flow in the maximum and minimum of the defect in the wake of the roughness and the comparison with the undisturbed flow in the normal coordinates are shown in Fig. 8. Here, the lines show an approximation of the experimental data. Since at height $y \approx 1$ mm defect of mean mass flow becomes close to zero for all sections, it can be concluded that in the wake of roughness element, the boundary layer thickness is not changed substantially. Here, the profiles at $z = 7.2$, 5.5, and 7.6 mm for the cases I, II, and III, respectively, and $z' = 4.2$ mm for the case IV correspond to the undisturbed flow. For the case I at $z = 0$ mm, at $z = 0.5$ mm for the cases II, III, and at $z' = 0.5$ mm for the case IV, the mean flow distortion is negative; therefore, in this position, the mass flow profile is less filled with respect to the undisturbed flow profile. At $z = -1.8$, -1.1, and -2 mm for the cases I, II, and III, respectively, and $z' = -1.4$ mm for the case IV, the mean flow distortion is positive; consequently, in this position, the mass flow profile is more filled. According to the stability theory, less filling of mass flow profile corresponds to a less flow stability, and larger filling of mass flow profile corresponds to a larger flow stability. From this, one can conclude that, in the wake of a sticker center, the flow is the most unstable. Moreover, Fig. 8 shows that the y-coordinate, at which the maximum positive mean flow distortion is observed, is smaller than the y-coordinate, at which the maximum negative defect appeared.

After the measurements in the near field of the roughness elements, it was obtained that the boundary layer thickness practically did not change. However, the level of natural disturbances inside the boundary layer is changed, and the pulsation evolution could be nonlinear. To check the nature of the pulsation evolution, the probability density distribution of waveform perturbations was performed for all the data points. Statistical analysis showed that the character of pulsation evolution did not change: it was linear for all configurations of the roughness element, except for a narrow region near $z = 0$ where the weak nonlinearity appeared.

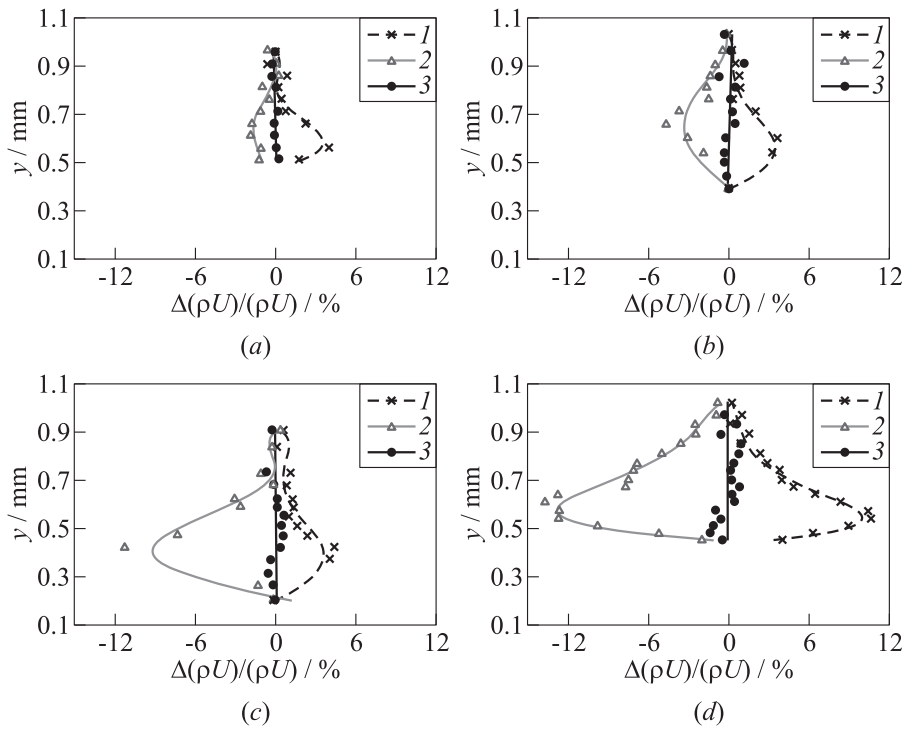

Figure 8 Profiles of mean flow distortion: (*a*) case *I*: *1* — $z = -1.8$ mm, *2* — 0, and *3* — $z = 7.2$ mm; (*b*) case *II*: *1* — $z = -1.1$ mm, *2* — 0.5, and *3* — $z = 5.5$ mm; (*c*) case *III*: *1* — $z = -2.0$ mm, *2* — 0.5, and *3* — $z = 7.6$ mm; and (*d*) case *IV*: *1* — $z' = -1.4$ mm, *2* — 0.5, and *3* — $z' = 4.2$ mm

A detailed understanding of the roughness effect on the natural fluctuation characteristics can be defined with the help of the analysis of their spectral characteristics. Figure 9 shows the power spectra of the natural disturbances in the boundary layer of smooth flat plate and flat plate with roughness elements for cases *I*, *II*, and *III*. Power spectral density of mass flow fluctuations $q_f = (\langle m_f \rangle)^2$ is given in relative units, with normalization to the mean mass flow of the incoming flow. In the case of a smooth flat plate, the natural disturbance spectra are practically the same for different values of the z-coordinates (see Fig. 9*a*), including the wake area behind aperture. Therefore, it can be concluded that the disturbance source inside the model was sealed, and the aperture for the disturbance generation into the boundary layer does not influence the natural disturbance spectra. For cases *I* and *II* (see Figs. 9*b* and 9*c*), the greatest influence on spectra appeared at the z-locations, corresponding to the maxima of the mean flow distortion (curves *2* and *4*). In these areas, the spectral power

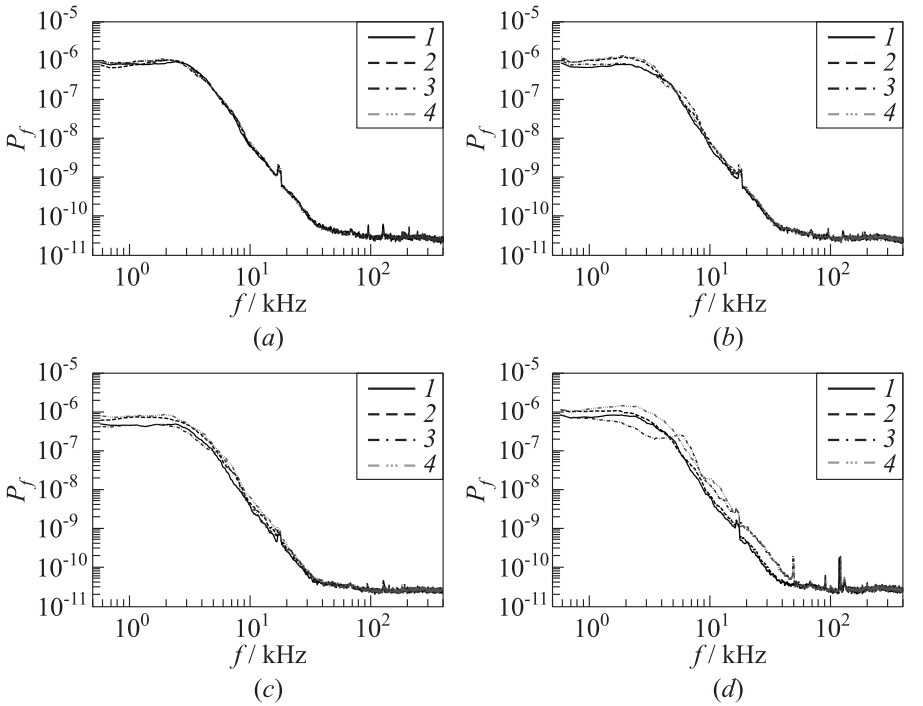

Figure 9 Power spectrum of fluctuations in the boundary layer: (*a*) the smooth surface of flat plate, *1* — $z = -6$ mm, *2* — -1.6, *3* — 0, and *4* — $z = 1.6$ mm; and (*b*)–(*d*) the configuration corresponds to the roughness elements *I*–*III*: *1* — undisturbed flow, *2* — first maximum, *3* — minimum, and *4* — second maximum. The coordinates of the maxima and minima are shown in Table 1

of the low-frequency perturbation is 1.5 times more than the one in undisturbed flow. However, in case *III* (Fig. 9*d*) when both the sticker and the aperture influence the mean flow, the power spectral density for the low-frequency part is approximately 2 times higher in the maxima of mean flow defect (curves *2* and *4*) and 2 times less in the minimum of mean flow defect (curve *3*) compared with the undisturbed flow (curve *1*).

Figure 10 shows the power spectral density of mass flow fluctuations in the boundary layer of the smooth swept wing and with roughness (case *IV*). From the data presented in Fig. 10*a*, it is clear that the spectral power of natural disturbances in the boundary layer of smooth swept wing is almost identical for different z-coordinates. Thus, similar to the case of smooth flat plate, the aperture does not influence the spectra. For case *IV* (Fig. 10*b*), the spectral power is different from the power spectrum of undisturbed flow for both the maxima and minima of the region across a wide band of frequencies.

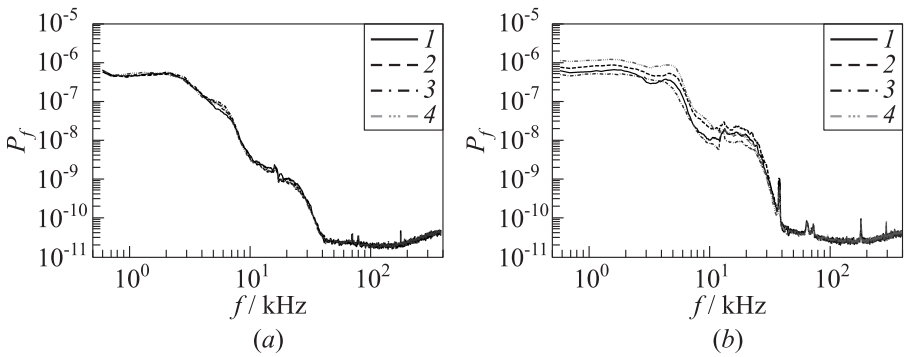

Figure 10 Power spectrum of fluctuations in the boundary layer: (a) the smooth surface of swept wing: *1* — $z' = -8$ mm, *2* — -1.5, *3* — 0, and *4* — $z' = 3$ mm; and (b) the configuration corresponds to the roughness element IV: *1* — undisturbed flow, *2* — first maximum, *3* — minimum, and *4* — second maximum. The coordinates of the maxima and minima are shown in Table 1

4 CONCLUDING REMARKS

The detailed experiments to evaluate the influence of flat isolated square and diamond shaped roughness elements on the mean and pulsation characteristics of the boundary layer on a flat plate and a swept wing have been conducted for the first time at Mach 2.

1. It is determined that the diamond-shaped sticker creates a larger mean flow defect in the normal to the surface direction compared with a flat square roughness, but the sticker shape almost has no effect on the absolute changes in mass flow pulsation distributions in the wake of the label.

2. It is obtained that the relative "receptivity" of the 3D boundary layer to stationary perturbations is approximately 1.5 times larger than the "receptivity" of 2D boundary layer.

3. It is found that the relative changes in mass flow pulsation distributions in the wake of a roughness element on the swept wing is in 1.5 times greater than in the flat plate boundary layer.

4. It is discovered that in the absence of roughness, the aperture in the surface has no influence to the spectral characteristics of natural disturbances. In the presence of labels on the line of aperture the spectra perturbations in 2Do and 3D boundary layers differ from the undisturbed spectra for both the maxima of mean flow defect region and the minimum one.

5. It is found that the flow is the most unstable in the wake of a sticker center.

ACKNOWLEDGMENTS

This work was partially supported by grants RFBR No. 13-01-00520.

REFERENCES

1. Laufer, J., and T. Vrebalovich. 1960. Stability and transition of a laminar boundary layer on an insulated flat plate. *J. Fluid Mech.* 9:257–299.
2. Kendall, J. M. 1975. Wind tunnel experiments relating to supersonic and hypersonic boundary-layer transition. *AIAA J.* 13(3):290–299.
3. Lebiga, V. A., A. A. Maslov, and V. G. Pridanov. 1979. Experimental investigation of the stability of supersonic boundary layer on a flat insulated plate. *J. Archives Mech.* 31(3):397–505.
4. Gaponov, S. A., and A. A. Maslov. 1980. *Disturbance development in compressible flows*. Novosibirsk: Nauka. 144 p. [In Russian.]
5. Zhigulev, V. N., and A. M. Tumin. 1987. *Turbulence origine*. Novosibirsk: Nauka. 282 p. [In Russian.]
6. Ermolaev, Yu. G., A. D. Kosinov, V. Ya. Levehenko, and N. V. Semenov. 1995. Instability of a three-dimensional supersonic boundary layer. *J. Appl. Mech. Tech. Phys.* 36(6):840–843.
7. Kosorygin, V. S., and N. F. Polyakov. 1990. Autodestruction of unstable waves of laminar boundary layer. *Bull. Am. Phys. Soc.* 35(10). 2291 p.
8. Saric, W. S., and H. L. Reed. 2002. Supersonic laminar flow control on swept wings using distributed roughness. AIAA Paper No. 2002-0147. 10 p.
9. Kachanov, Yu. S., V. V. Kozlov, and V. Ya. Levchenko. 1982. *Origin of turbulence in boundary layer*. Novosibirsk: Nauka. 151 p. [In Russian.]
10. Kosinov, A. D., A. A. Maslov, and S. G. Shevelkov. 1990. Experiments on the stability of supersonic laminar boundary layers. *J. Fluid Mech.* 219:621–633.
11. Kosinov, A. D., N. V. Semionov, and S. G. Shevelkov. 1994. Investigation of supersonic boundary layer stability and transition using controlled disturbances. *ICMAR-94 Conference Proceedings*. 2:159–166.
12. Gaponov, S. A., and I. I. Maslennikova. 1997. Subharmonic instability of supersonic boundary layer. *J. Thermophys. Aeromech.* 4(1):10–17.
13. Ermolaev, Yu. G., A. D. Kosinov, and N. V. Semenov. 1997. An experimental study of the nonlinear evolution of instability waves on a flat plate for Mach number M = 3. *J. Appl. Mech. Tech. Phys.* 38(2):265–270.
14. Mayer, C., and H. F. Fasel. 2008. Investigation of asymmetric subharmonic resonance in a supersonic boundary layer at Mach 2 using DNS. AIAA Paper No. 2008-0591. 25 p.
15. Kosinov, A. D., N. V. Semionov, and V. G. Yermolaev. 2010. Experiments on the wave train excitation and wave interaction in spanwise modulated supersonic boundary layer. *7th IUTAM Symposium on Laminar–Turbulent Transition Proceedings*. Heideberg: Springer. 18:513–516.
16. Duan, L., X. Wang, and X. Zhong. 2013. Stabilization of a Mach 5.92 boundary layer by two-dimensional finite-height roughness. *AIAA J.* 51(1):266–270.

17. Zhong, X., and X. Wang. 2012. Direct numerical simulation on the receptivity, instability, and transition of hypersonic boundary layers. *Annu. Rev. Fluid Mech.* 44:527–561.
18. Radeztsky, Jr., R. H., M. S. Reibert, and W. S. Saric. 1999. Effect of isolated micron-sized roughness on transition in swept-wing flows. *AIAA J.* 37(11):1371–1377.
19. Reshotko, E. 2001. Transient growth A factor in bypass transition. *Phys. Fluids* 13(5):1067–1075.
20. Tumin, A., and E. Reshotko. 2001. Spatial theory of optimal disturbances in boundary layers. *Phys. Fluids* 13(7):2097–2104.
21. Fransson, J. H. M., L. Brandt, A. Talamelli, and C. Cossu. 2004. Experimental and theoretical investigation of the nonmodal growth of steady streaks in a at plate boundary layer. *Phys. Fluids* 16(10):3627–3638.
22. Fransson, J. H. M., A. Talamelli, L. Brandt, and C. Cossu. 2006. Delaying transition to turbulence by a passive mechanism. *Phys. Rev. Lett.* 96:064501.
23. Semionov, N. V., and A. D. Kosinov. 2007. Method laminar–turbulent transition control of supersonic boundary layer on a swept wing. *J. Thermophys. Aeromech.* 14(3):337–341.
24. Groskop, G., M. J. Kloker, K. A. Stephani, O. Marxen, and G. Iaccarino. 2010. Hypersonic flows with discrete oblique surface roughness and their stability properties. *2010 Summer Program Proceedings.*
25. Fransson, J. H. M., B. E. G. Fallenius, S. Shahinfar, S. S. Sattarzadeh, and A. Talamelli. 2011. Advanced fluid research on drag reduction in turbulence experiments. *J. Phys.: Conference ser.* 318:032007.
26. Schneider, S. P. 2008. Effects of roughness on hypersonic boundary-layer transition. *J. Spacecraft Rockets* 45(2):193–209.
27. Semionov, N. V., A. D. Kosinov, and V. Y. Levchenko. 2006. Experimental study of turbulence beginning and transition control in a supersonic boundary layer on swept wing. *6th IUTAM Symposium on Laminar–Turbulent Transition Proceedings.* 78:355–361.
28. Panina, A. V., A. D. Kosinov, Yu. G. Yermolaev, and N. V. Semionov. 2010. Investigation of influence of spanwise flow nonuniformity on controlled disturbances evolution in supersonic boundary layer. *J. Vestnik of the NSU. Physics* 5(2):17–27. [In Russian.]
29. Kosinov, A. D., G. L. Kolosov, A. V. Panina, N. V. Semionov, and Yu. G. Yermolaev. 2013. Experiments on relative receptivity of three-dimensional supersonic boundary layer to controlled disturbances and its development. *Progress in flight physics.* Eds. Ph. Reijasse, D. D. Knight, M. S. Ivanov, and I. I. Lipatov. EUCASS advances in aerospace sciences book ser. TORUS PRESS–EDP Sciences. 5:69–80.
30. Kosinov, A. D., N. V. Semionov, and Yu. G. Yermolaev. 1999. Disturbances in test section of T-325 supersonic wind tunnel. Novosibirsk: Siberian Branch of the Russian Academy of Sciences, Institute of Theoretical and Applied Mechanics. Preprint 6-99. 24 p.
31. Kosinov, A. D., and A. I. Semisynov. 2003. Character of evolution of natural disturbances in a supersonic boundary layer on a flat plate. *J. Thermophys. Aeromech.* 10(1):39–44.
32. Smits, A. J., K. Hayakawa, and K. C. Muck. 1983. Constant temperature hot-wire anemometer practice in supersonic flows. *Exp. Fluids* 1:83–92.